https://doi.org/10.48047/AFJBS.6.5.2024.1371-1389

African Journal of Biological Sciences

Journal Homepage: http://www.afjbs.com

Research Paper Open Access

Green Synthesis of *Guaiacum officinale* L. Bark Extract Silver Nanoparticles Enhanced Anticancer Activity in Human Bone Marrow Neuroblastoma Cancer Cells

Rangavitala, P. and Taranath, T. C.*

Environmental Biology and Green Nanotechnology Laboratory, P. G. Department of Studies in Botany, Karnatak University, Dharwad – 580 003, Karnataka, India.
*Corresponding author: tctaranath@gmail.com

Article History

Volume 6, Issue 5, Apr 2024

Received: 23 March 2024

Accepted: 28 April 2024

Published: 04 May 2024

doi:10.48047/AFJBS.6.5.2024.1371-1389

ABSTRACT

The ultrasonically-assisted hydroacetonic *Guaiacum officinale* L. bark extract (GoBE) was used to synthesize the AgNPs. The phytochemicals in the bark extract act as major capping and reducing agents and the synthesized AgNPs were investigated for in-vitro antioxidant and anticancer activities. The colour change of the reaction mixture from light brown to dark brown represents the synthesis of *Guaiacum officinale* bark extract silver nanoparticles (GoBE-AgNPs). An absorption peak at 410 nm was checked by UV-vis spectrophotometer. FTIR reveals functional group participation in AgNPs capping. Powder XRD and SAED validated the crystallinity and ~20–27 nm size with spherical-shaped AgNPs were observed in HR-TEM images. The EDS showed the presence of elemental silver. In DLS spectral analysis, the zeta potential was measured at -42.2 mV and the particle size analyzer validated the hydrodynamic size of +40.7 nm. Dose-dependent DPPH radical scavenging activity showed a 94.62±0.015% inhibition. GoBE-AgNPs were treated with Human bone marrow neuroblastoma (SH-SY5Y) cancer cell lines at 12.5 to 200 µg/mL concentrations. The MTT assay showed 44.85±0.017% cell viability. Annexin V/FITC assay revealed 59.49% apoptosis in cancer cells. AgNPs generated 33.88% oxidative stress in SH-SY5Y cells. The current research ensured the effective antioxidant and anticancer activity of GoBE-AgNPs.

Keywords: Anticancer, Apoptosis, Green synthesis, *Guaiacum officinale* L., Silver nanoparticles, Ultrasonic-assisted extraction

1. Introduction

Nanotechnology is a branch of science, and it has become a multidisciplinary field which covers several areas like chemistry, physics, biology, medicine, and pharmaceuticals, and are increasing further interest in the synthesis of nanoparticles (NPs) (Boholm and Arvidsson, 2016). Due to the potential applications in different biological activities and relatively cost-effective with unique physicochemical properties, silver nanoparticles (AgNPs) possess an exceptional preference for metallic nanoparticles (Arya et al., 2018). To create AgNPs, a wide variety of traditional and unconventional techniques are used. Traditional approaches are incredibly costly, energy-intensive, and chemically harmful. In response to these concerns, innovative environmentally conscious green synthesis techniques have been developed for the production of AgNPs through plant-based processes (Chandra et al., 2020).

The phytoconstituents are found in the plants and they serve as capping materials. There were multiple reports of efforts to environmentally synthesize AgNPs using crude plant extracts. (Narayanan and Sakthivel, 2011). The plant extract has been prepared by an effective and rapid extraction technique that is the ultrasonicator-assisted extraction (UAE) method, which is the most efficient and more appropriate in saving time consumption, cost reduction, and resulting in a high yield of extract (Syahir et al., 2020). The hydroacetonic bark extract of the Zygophyllaceae family plant *Guaiacum officinale* L. (Lignum vitae) was used to examine the formation of AgNPs. Several studies reported that resins and extracts of *Guaiacum officinale* were treated for anti-inflammatory properties and efficient activity against arthritis, and sciatica conditions. As a rich resource of saponins, bark, leaves, and flowers contain saponins like guaianin and guaiacin which are used as an immunostimulant, membrane-permeabilizing, and hypocholesterolemic properties (Ahmed et al., 2012). Hence, *Guaiacum officinale* bark extract (GoBE) was utilized for the green synthesis of AgNPs. The parameters like the ratio of extract to AgNO3, the concentration of AgNO3, temperature, pH, and the amount of time spent in the reaction mixture play an important role in nanoparticle synthesis (Hulkoti & Taranath, 2014).

Additionally, the most esoteric and deadly form of pediatric cancer that develops a solid carcinogenic tumor that starts to grow in the nerve cells outside the brain in the neurological system of young children and is known as human bone marrow neuroblastoma cancer (Jyoti D et al., 2022). Hence, GoBE-AgNPs were tested against human bone marrow neuroblastoma cancer (SH-SY5Y) cell lines.

2. Materials and methods

2.1. Collection, authentication and extraction of GoBE

Fresh bark of *Guaiacum officinale* L. was collected from Railway quarters, near the Gadag Railway station, Gadag, Karnataka, India - 582101. The collected bark samples were critically examined for morphological, microscopic observable characteristics. Professor K. Kotresha, Postgraduate Department of Botany at Karnataka Science College, Dharwad, Karnataka, India – 580001, provided vital specimen identification and verification in addition to the factual information that was required. The collected bark samples were cleaned with Milli-Q water to get rid of any contaminants and let to dry at room temperature for fifteen days in the shade. A fine powder was produced by pulverization. Using Milli-Q water and 70% acetone (hydroacetone) (1:8 w/w) in a 1L autoclavable bottle with an air condenser and utilizing the direct sonication method (Sulaiman et al., 2011; Pandhari and Taranath, 2024) and optimizing it according to the needs, an ultrasonicator-assisted extraction (UAE) was performed using Athena Multifunctional Ultrasonicator Cleaner bath model (ATS-10L). The total percentage of yield was calculated using the formula:

$$\% \text{ Yield} = \frac{\text{Weight of the extract}}{\text{Weight of the plant material}} \times 100$$

2.2. Green synthesis and characterization of GoBE-AgNPs

A 5 g of hydroacetonic bark extract was mixed with 50 mL of Milli-Q water. A solution of 1 mM aqueous $AgNO_3$ and 5 mL of diluted aqueous bark extract were combined to reduce the silver ions. The mixture was incubated at 25 ℃ for 6 hours and adjusted to pH 10 with 1 N NaOH and agitated for 10 min. Synthesized silver nanoparticles were diluted with Milli-Q water in 1:7 ratio and a double-beam UV-Vis spectrophotometer (JASCO UV-VIS NIR V-670) with 300-800 nm wavelength was used to record the absorption spectra. AgNPs were purified by centrifugation at 5000 rpm for 15 min. using a REMI Cooling C-24 BL Centrifuge. Washed the reaction mixture thrice with Milli-Q water and supernatant was discarded and the concentrated slurry was collected and air-dried for further analyses. Following the preparation of KBr pellets with purified AgNPs and FTIR analysis was carried out using a Thermo-Fischer Scientific Nicolet 6700 analyzer with a resolution of 4 cm^{-1} and 500-4000 cm^{-1} wavelength. A powder X-ray diffractometer (RIGAKU Smartlab SE) equipped with Cu Kβ (1.3923 Å) radiation, 40 kV, 30 mA current, 5~90° diffraction angle and 10.00°/min scanning rate was used to determine the crystallinity of silver nanoparticles. High resolution-transform microscopy (HR-TEM), Selected area electron diffraction

(SAED) and Energy dispersive spectroscopy (EDS) was performed using Thermo-Fischer, TALOS F200 G2 instrument to check the size, shape, orientation and crystallinity of synthesized AgNPs. Purified AgNPs were mixed with Milli-Q water to prepare the hydrodynamic solution, further, the dynamic light scattering (DLS) (HORIBA SZ-100) spectral analysis was performed to investigate the zeta potential and particle size distribution of synthesized AgNPs in aqueous medium.

2.3. Antioxidant capacity of GoBE-AgNPs

DPPH (2,2-diphenyl-1-picrylhydrazyl) free radical scavenging activity was performed according to the method developed by Salari et al (2019). Briefly, the combination of 3 mL of methanol and 5 mL of 0.1 mM DPPH solution was mixed with different concentrations (12.5, 25, 50, 100, 200 ug/mL) of GoBE-AgNPs. After proper stirring, the solutions were kept in the dark for 30 min. Ascorbic acid was used as the standard and 517 nm absorbance was recorded using UV-Vis Spectrophotometer. The percentage of DPPH activity was calculated using the formula: [(Ac – As) / Ac] × 100, where 'As' represents the absorbance of the sample and 'Ac' represents the absorbance of the control. The IC_{50} value determines the potentiality of the drug.

2.4. Anticancer activity of GoBE-AgNPs

Cell culture conditions: The Human bone marrow neuroblastoma cancer (SH-SY5Y) cell lines were obtained from the National Centre for Cell Sciences (NCCS), Pune, India. The cell lines were cultured on a petri dish using 10 % fetal bovine serum (#RM10432, Himedia) and high glucose DMEM (#AL111, Himedia), placed in a CO_2 incubator (Heal Force, China) at 37 ℃ temperature and 5 % humidified atmospheric CO_2. Subculturing was done every 24 hours. A 96-well plate (Corning, USA) was seeded with 200 µl of cell suspension, with 20,000 cells per well. After this, the plate spent 24 hours with 5% CO_2 and 37 ℃ temperature in an incubator

Assay Controls: Positive control: Cancer cells treated with Camptothecin in a culture medium. Control group: Cancer cells cultured in media devoid of experimental drug. Cells treated with GoBE-AgNPs in 0.1 % DMSO at different concentrations served as the test group.

MTT [3-(4,5-Dimethylthiazol-2-yl)-2,5-Diphenyltetrazolium bromide] assay: SH-SY5Y cells were treated with GoBE-AgNPs and standard camptothecin (#C9911, Sigma-Aldrich) after 24 hours of incubation. Immediately after the medium was removed, 0.5 mg/mL of MTT reagent (#4060 HiMedia) and 100 µL of solubilization solution DMSO (dimethyl sulfoxide) (#PHR1309, Sigma-Aldrich) were added into the mixture. Following the dissolution of MTT formazan crystals in DMSO, absorbance was recorded at 570 nm (Alley et al., 1986). The percentage of cell viability was calculated using the formula:

$$\text{Cell viability (\%)} = \left(\frac{\text{Mean absorbance of treated cells}}{\text{Mean absorbance of untreated cells}}\right) \times 100$$

The IC_{50} value was calculated by using a linear regression equation Y=Mx+C.
Where, Y = 50, M and C values were derived from the viability graph.

Apoptotic assay by flow cytometry: A 6-well plate was used to culture human bone marrow neuroblastoma (SH-SY5Y) cells at a density of $0.5x10^6$ cells/2 mL. Immediately after being exposed to GoBE-AgNPs and standard camptothecin at IC_{50} concentrations for 24 hours of incubation, removed the media and washed the cells with PBS and 200 µL of trypsin-EDTA was added and incubated at 37 ℃ for 3-4 minutes. The cell lines were collected and placed straight into polystyrene tubes measuring 12x75 mm, and 2 mL of growth medium was added to each tube. Following a 5-minute centrifugation at 300 x g at 25 ℃, the cells were washed twice in PBS. Also, the supernatant was carefully drained off after the centrifugation. By gently vortexing the sample, 5 µL of FITC Annexin V (#51-65874X, BD-Biosciences) was added and incubated for 15 min. at 25 ℃ in the dark. After adding 400µl of 1X binding buffer and 5 µL of PI (Propidium iodide) (#51-66211E, BD-Biosciences), each tube was gently vortexed (Koopman et al., 1994). The fluorescence-activated cell sorting (FACS) technique was used for the analysis of cell apoptosis.

Determination of ROS Generation: SH-SY5Y cell lines were cultured as previously (Koopman et al., 1994). To prepare a 10 µM working solution, H2DCFDA (2', 7'-dichlorodihydrofluorescein diacetate indicator (#D-399, Life Technologies, Invitrogen) (4mM in DMSO) was diluted with DPBS (#TL1006, HiMedia). SH-SY5Y cells encapsulated with GoBE-AgNPs were suspended in the H2DCFDA indicator at a concentration of 1×10^6 cells/mL. Incubated for 30 minutes at 37 ℃ and centrifuged at 150 x g for 5 minutes. Removed the supernatant and gently resuspended cells in the 400µl pre-warmed DPBS were evaluated for the DCF (2', 7'-dichlorofluorescein) intensity using flow cytometry (BD

Biosciences FACS Calibur, CA, USA) at a wavelength of 488 nm for excitation and 535 nm for detection via the FL1 channel (Behera and Awasthi, 2021).

Statistical analysis: All the experiments were performed in triplicates (n = 3), and the data were produced as the mean ± standard deviation.

3. Results

3.1. Total yield of UAE crude extract

9.5 g of hydroacetonic crude extract was produced from 30 g of *Guaiacum officinale* bark powder using an ultrasonic-assisted extraction method and the total percentage of yield was 31.66% w/w.

3.2. Characterization of synthesized GoBE-AgNPs

UV- Vis spectroscopic analysis: The synthesis of AgNPs was visually confirmed by the color change from a clear pale brown to dark brown color and synthesized AgNPs at pH 10 showing a clear UV-vis absorption peak at 410 nm (figure 1).

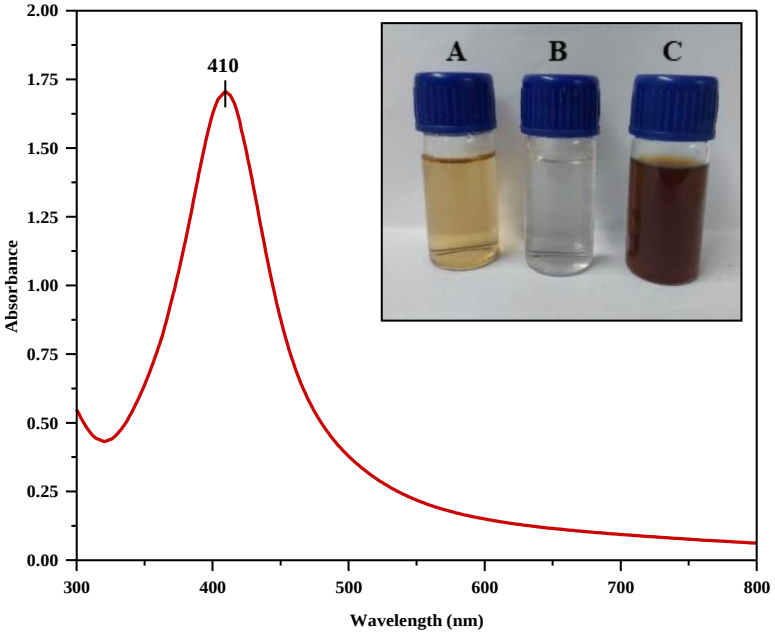

Fig. 1. UV-vis absorption spectra of GoBE-AgNPs at pH 10. (A) Bark extract (B) 1mM $AgNO_3$ (C) Reaction mixture

Fourier transform infrared (FTIR) Analysis: FTIR data of GoBE-AgNPs determined that the C-H aldehydic stretching was observed at 3417.43 cm^{-1} and shift from 2923.77-2857.89 cm^{-1}. The medium stretching peaks at 1599.70 cm^{-1} and 1513.65 cm^{-1} indicating the existence

of amines (composed of the N-H group) and nitro (composed of the N-O group) compounds respectively. A stretching peak at 1384.37 cm^{-1} was associated with the O-H group. The vibrational stretch of -C-O originates from the polyols, were assigned at 1070.05 cm^{-1}. An aromatic C=C alkenes was indicated by an absorption peak at 872.72 cm^{-1} (Figure 2).

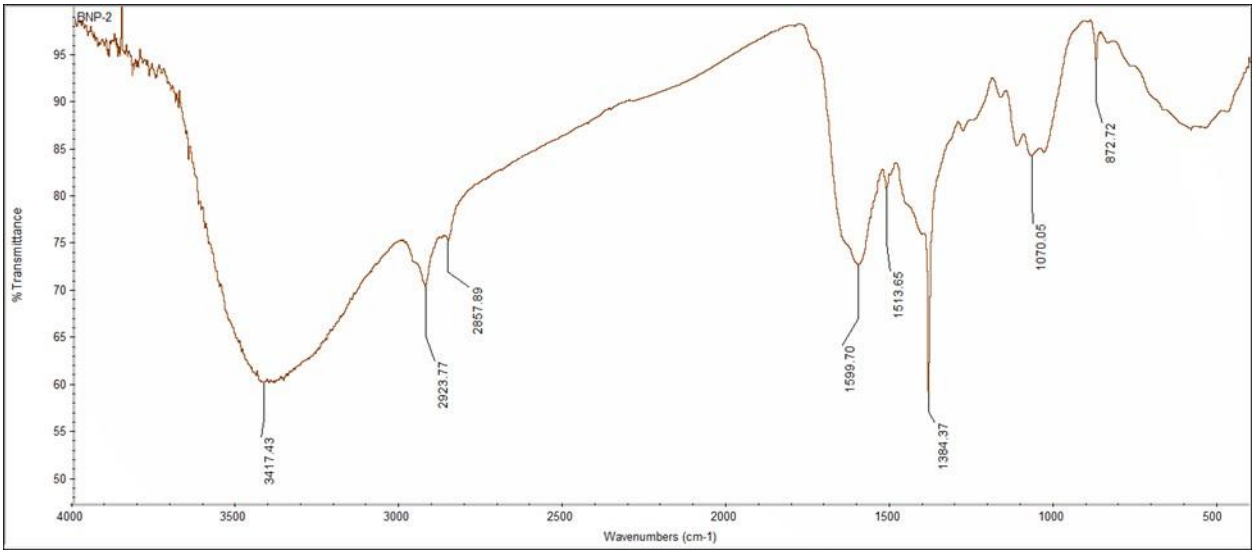

Fig. 2. FTIR spectra of GoBE-AgNPs

Powder X-ray powder diffraction (XRD): The results of GoBE-AgNPs showed that the miller indices at (111), (200), (220), (311), and (222) correlate to the Bragg peaks (2θ angle) at 38.13°, 44.29°, 64.46°, 77.40°, and 81.61°, respectively. The ICDD Card 00-004-0783 indexed face-centered cubic (FCC) structure of crystalline nature of AgNPs and an average size of ~14.43 nm was determined using Scherer's equation. (Figure 3).

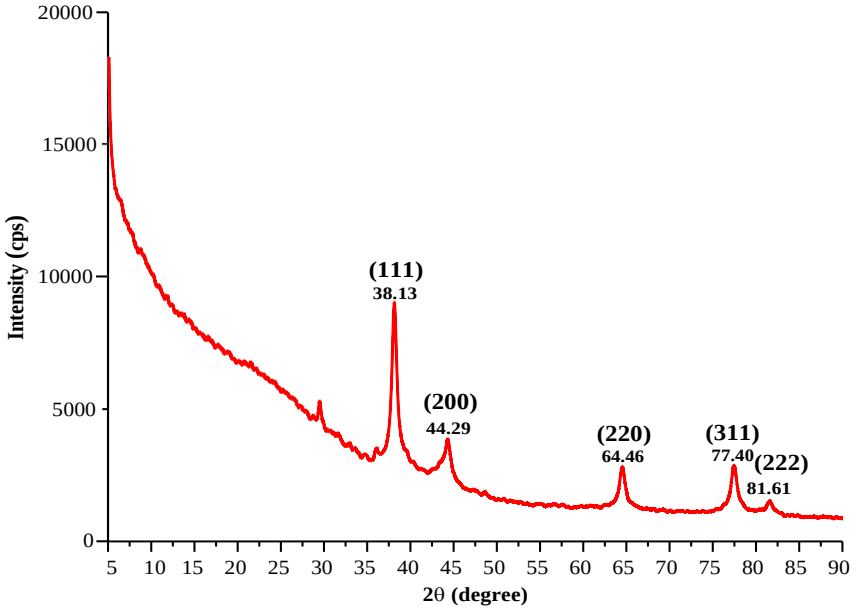

Fig. 3. Powder XRD pattern of GoBE-AgNPs

HR-TEM, SAED and EDS study: HR-TEM study confirms the shape and size of synthesized AgNPs as smooth-edged, spherical-shaped with polydispersed and size ranges from 20-27 nm in diameter (Figure 4 A-D). The clear bright spots from Bragg's reflection confirm the obtained nanoparticles were extremely crystalline as shown in SAED pattern (Figure 4E). A strong signal of elemental silver peak at 3 keV confirmed by EDS analysis (Figure 4F).

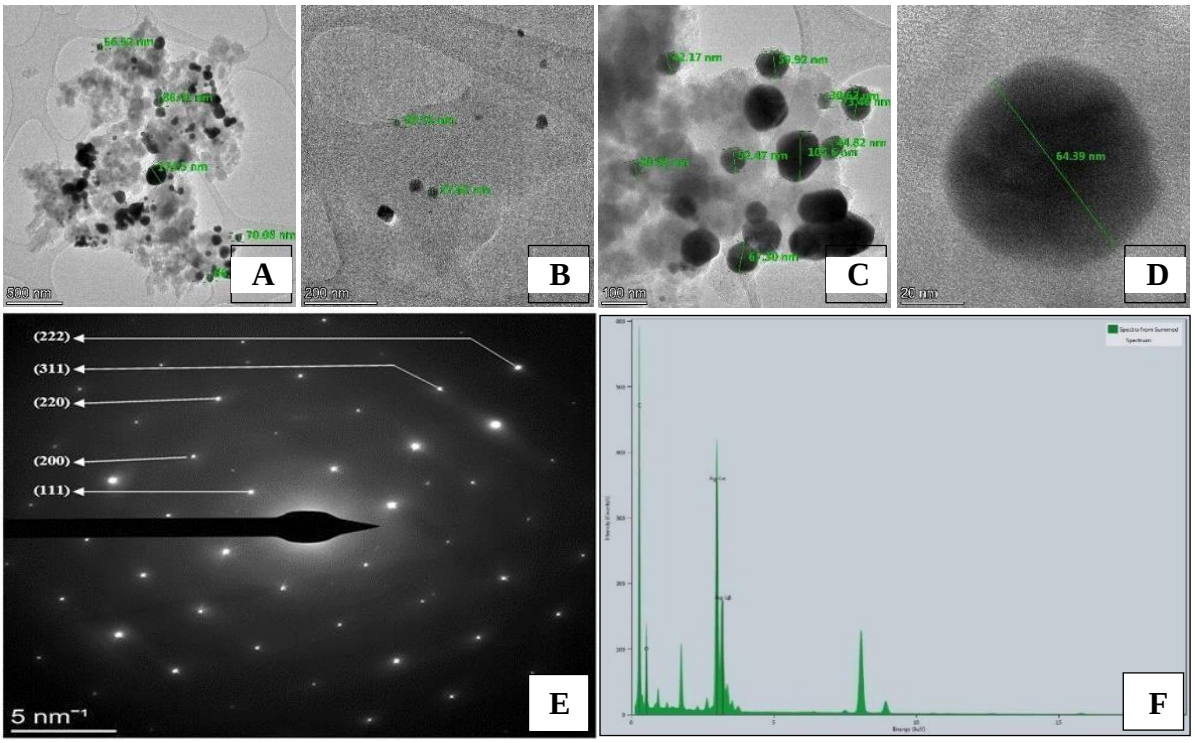

Fig. 4. HR-TEM images of GoBE-AgNPs. Different sized AgNPs (A) 500 nm, (B) 200 nm, (C) 100 nm, (D) 20 nm along with (E) SAED pattern and (F) EDS spectrum

Dynamic light scattering (DLS) spectral analysis: The synthesized GoBE-AgNPs were examined for surface zeta potential, polydispersity index and hydrodynamic size. As depicted in Figure 5A, the surface zeta potential was found to be -42.2 mV. The polydispersity index was 0.684 and hydrodynamic size was +40.7 nm. (Figure 5B).

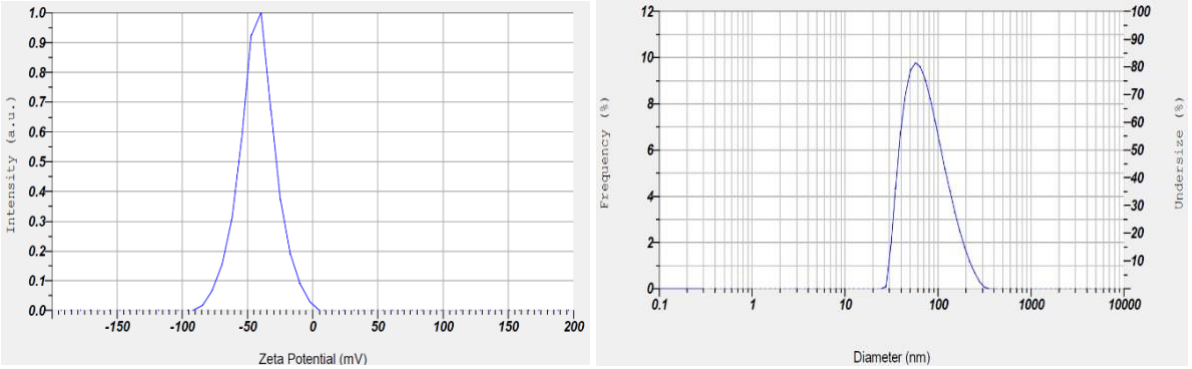

Fig. 5. DLS spectrum showing (A) Surface zeta potential and (B) Particle size distribution

3.3. DPPH mediated antioxidant activity

The dose-dependent DPPH radical scavenging ability of GoBE-AgNPs was 94.62±0.015% and that of the standard ascorbic acid was 93.74±0.067% at 200 µg/mL concentrations (Figure 6). In Table 1, the IC_{50} value of AgNPs was found to be 50.91 µg/mL, while the standard value was 35.39 µg/mL.

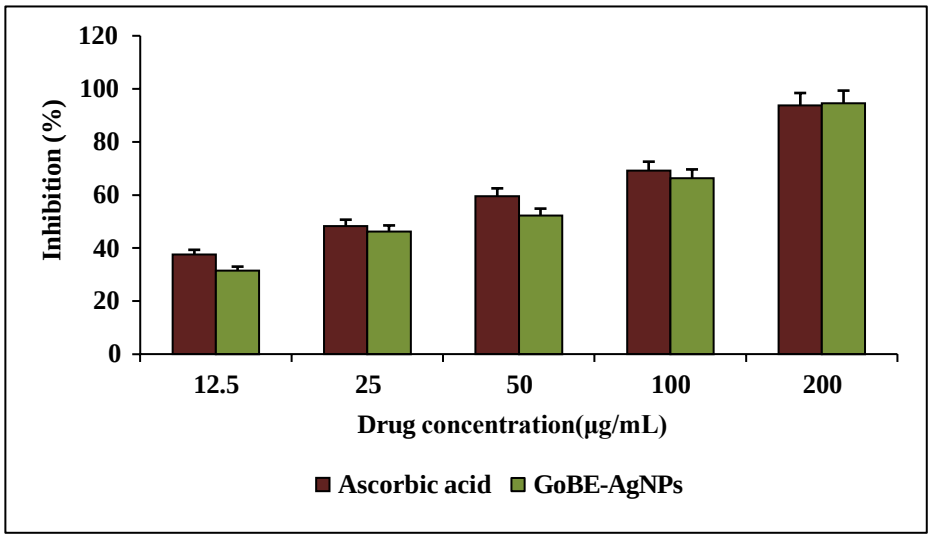

Fig. 6. Comparison graph of DPPH radical scavenging activity between standard ascorbic acid and GoBE-AgNPs.

Table1.Comparative % DPPH inhibition between standard ascorbic acid and GoBE-AgNPs with IC_{50} concentration

Concentration (µg/mL)	Percentage inhibition (%)	
	Ascorbic acid	GoLE-AgNPs
12.5	37.53±0.026	31.51±0.019
25	48.30±0.057	46.24±0.009
50	59.52±0.073	52.27±0.006
100	69.09±0.018	66.35±0.016
200	93.74±0.067	94.62±0.015
IC_{50} (µg/mL)	35.39	50.91

Data expressed as mean ± standard deviation (n = 3)

In-vitro Anticancer activity

Cell viability assay: The effect of GoBE-AgNPs on SH-SY5Ycells was determined by the MTT cell viability experiment. The results showed that the cell viability of camptothecin was 44.85±0.017% and GoBE-AgNPs was 49.19±0.022% at 200 µg/mL concentration (Figure 7). Figure 8 depicts the important morphological variations like membrane blabbing and shrinkage of cancer cells. The IC_{50} values of camptothecin and GoBE-AgNPs was found to be 195.26 µg/mL and 172.81 µg/mL respectively (Table 2).

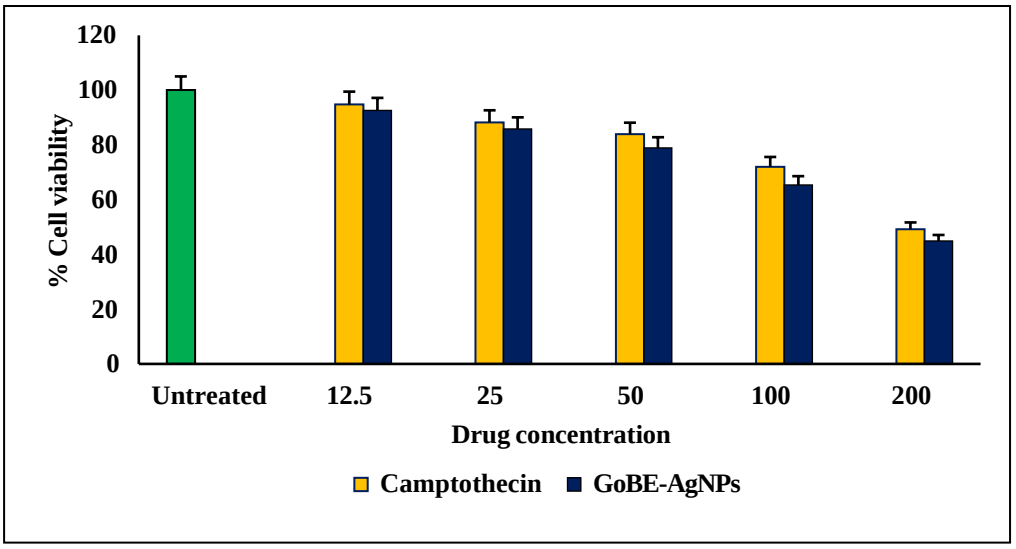

Fig. 7. Percentage cell viability of camptothecin and GoBE-AgNPs against SH-SY5Y cells after the 24 hours of incubation

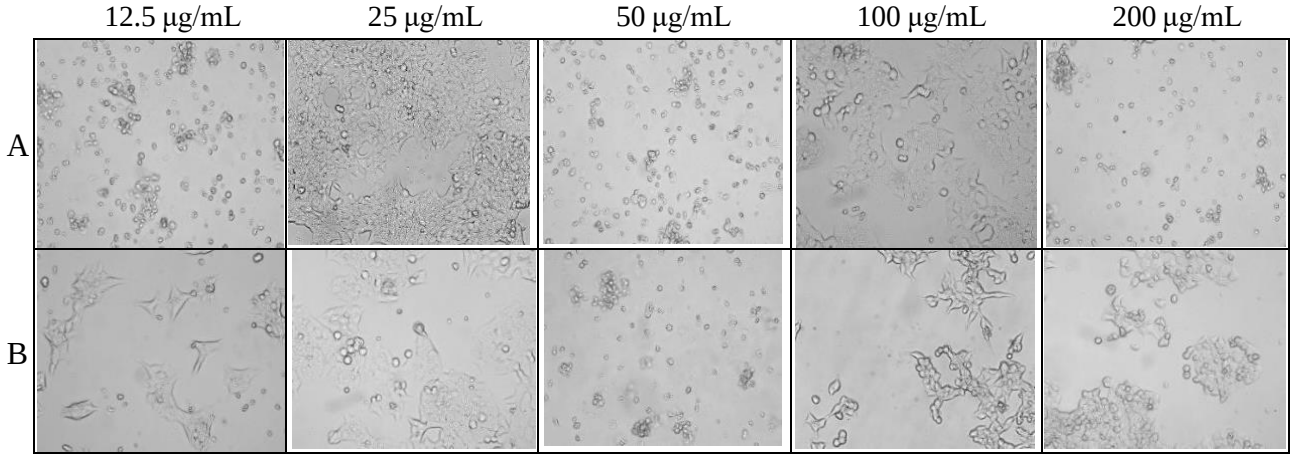

Fig. 8. Microscopic images of MTT cell viability assay (A) SH-SY5Y cells treated with Camptothecin, (B) SH-SY5Y cells treated with GoBE-AgNPs

Table 2. IC_{50} concentrations of camptothecin and GoBE-AgNPs in µg/mL

Cell line	Camptothecin	GoBE-AgNPs
SH-SY5Y	195.26	172.81

GoBE-AgNPs caused Apoptosis in SH-SY5Y cells: The inhibitory action of GoBE-AgNPs on the SH-SY5Y cells was evaluated using propidium iodide (PI) and double-marked Annexin V FITC stains, together with FACS flow cytometry. Figures 9 and 10 demonstrated the rate of apoptosis in SH-SY5Y cells increased from 3.63% (Untreated) to 52.83% (standard) and 59.49% (GoBE-AgNPs) and following a 24-hour exposure to IC_{50} concentrations of AgNPs and Camptothecin.

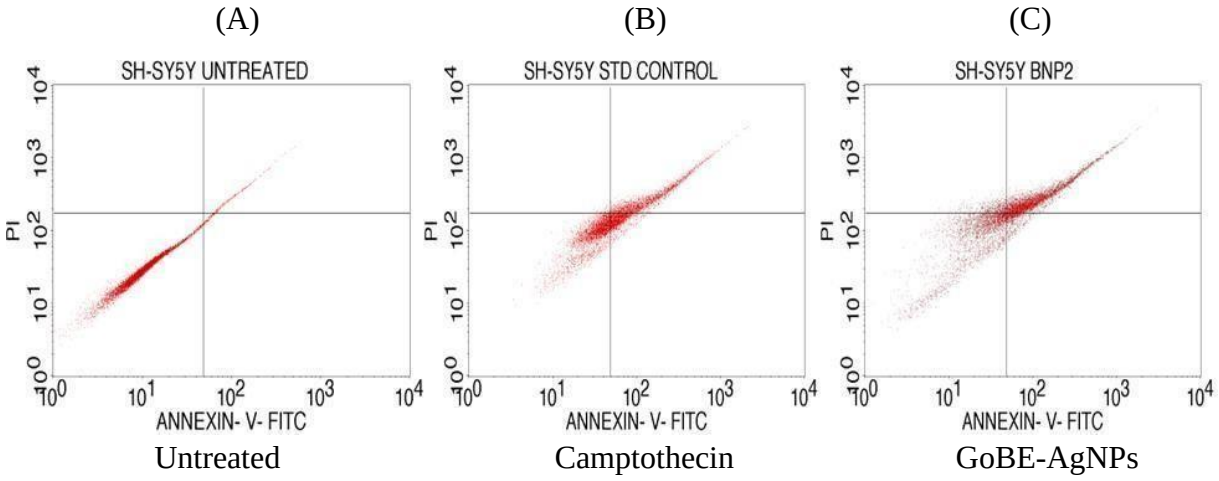

Fig. 9. Annexin V FITC/PI expression in SH-SY5Y cells (A) Untreated SH-SY5Y cells, (B) Camptothecin treated SH-SY5Y cells, (C) GoBE-AgNPs treated SH-SY5Y cells

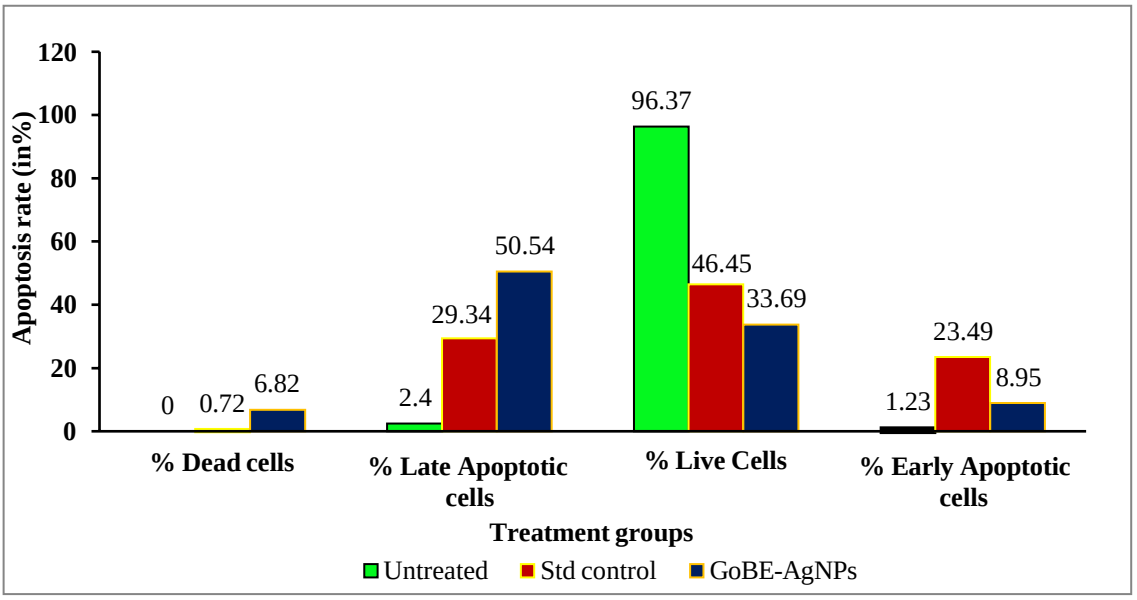

Fig.10.The percentage of Apoptotic and Necrotic cells in SH-SY5Y cells

ROS generation of GoBE-AgNPs: The results demonstrated that the IC_{50} concentration of camptothecin and GoBE-AgNPs the control both greatly increased ROS production in SH-SY5Y cells.While the ROS generation in SH-SY5Y cells was 0.53% in untreated cells, it was 49.01% in camptothecin cells, and 33.88% in GoBE-AgNPs cells (Figure 11). Thus, when compared with untreated-SH-SY5Y cells the synthesized AgNPs showed 63.92-fold increase in ROS generation (Figure 12).

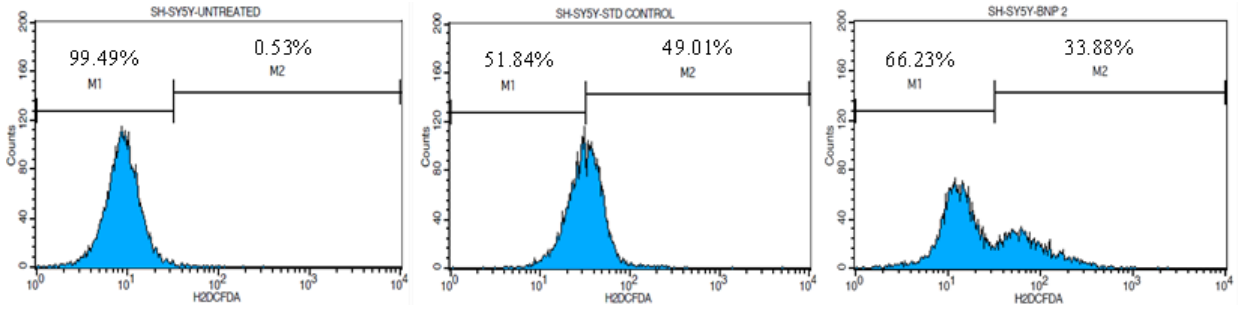

(A) **(B)** **(C)**

Fig. 11. H2DCFDA expression study of (A) Untreated SHSY-5Y cells, (B) Camptothecin treated SH- SY5Y cells and (C) GoBE-AgNPs treated SH-SY5Y cells

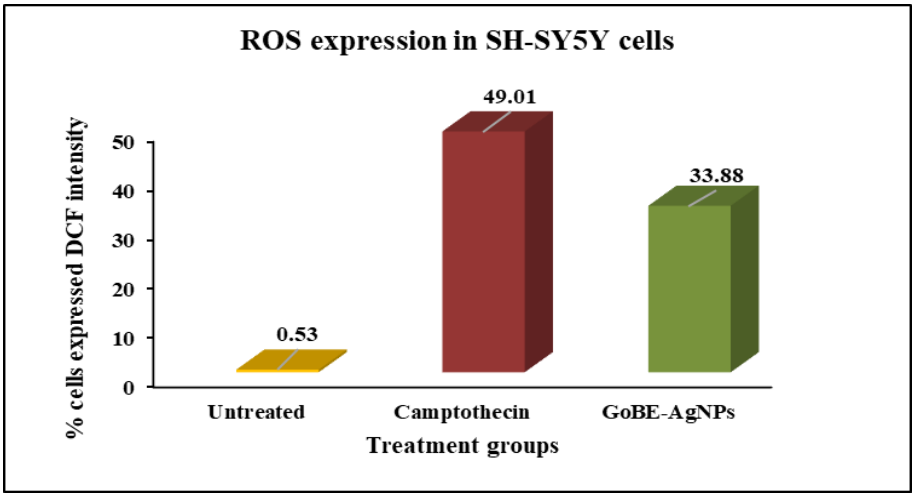

Fig. 12. Percentage of SH-SY5Y cells expressed DCF intensity in different treatment groups

3. Discussion

Nanoparticles have rich potential in different fields like water purification, pollution control, laser technology, nano-forensics, etc. for the betterment of mankind. Among many other kinds, silver nanoparticles have found widespread use. The AgNPs were normally synthesized by photochemical reduction, laser ablation, electrochemical reduction, and chemical reduction methods (Abou El-Nour et al., 2010). It is not always the case that these methods are good for the environment. Hence, in recent years have seen the development of alternative green synthesis, which aims to lessen or do away with the use of toxic compounds and prevent their

intervention. The green synthesis process starting to gain popularity as a result of concerns regarding health, the economy, and the environment. The current research investigated the eco-friendly synthesis of AgNPs by employing a hydroacetonic bark extract from *Guaiacum officinale* and their antioxidant and anticancer properties were evaluated in-vitro against SH-SY5Y cells.

UAE method employed ultrasound which facilitates cell disruption to discharge intracellular materials. According to a study by Teng et al. (2010), using ultrasound increased productivity. Ultrasound has long been recognized to accelerate the expansion and implosive collapse of water bubbles in addition to cavitation, due to which the reaction time was reduced and the extraction yield was increased. For 30 g of bark powder in hydroacetonic solvents at a material-to-solvent ratio of 1:8, maintained at a temperature of 60 ℃ boiling point, the overall percentage of yield was 31.66% w/w crude extract. The crude extract contains bioactive compounds that aid in the reduction, capping, and stability of AgNPs, and the antioxidant and anticancer therapies are influenced by bioactives derived from the UAE (Ravichandra et al., 2018).

As part of the environmentally friendly synthesis of AgNPs, the concentration, pH, temperature, and incubation time are some of the experimental factors that are involved. A shift in hue occurred from light brown to dark brown when nanoparticles were synthesized. Surface plasmonic resonance (SPR) waves induced in the water-based solution, which led to the development of color and absorption of the substance. Using a UV-Vis spectrophotometer, the SPR peak was observed at 410 nm providing evidence that the synthesis of AgNPs was carried out accurately. (Hulkoti & Taranath, 2014).

The functional groups implicated as reducing and capping agents were identified using FT-IR measurement, which was used for further characterization. The different absorption peaks seen in Figure 2, which represent the O-H group that is created when silver ions bind to hydroxyl groups, verified the presence of polyphenols and enhanced the stability of nanoparticles. GoBE-AgNPs had various bioactives, including aldehydic (C-H) groups, amines (N-H), nitro (N-O) compounds, polyols (-C-O), and aromatic C=C alkenes found in the bark extract (Xu et al., 2013).

Figure 3 depicts the powder X-ray diffractogram of silver nanoparticles. At 38.13° corresponding to 111 plane indicated that a more predominant crystallographic nature due to presence of higher atom density enhanced the particle size along with orientation (Nhung & Lee, 2014).

By Debye-Scherrer equation, $D = K\lambda/\beta cos\ \theta$ to determine the crystalline size of nanoparticles. The diffraction peak at full-width half maximum (FWHM)(β), the wavelength of the X-ray (λ), the Scherrer's constant (K), the crystal size (D), and the Bragg's angle (θ) are all entities that are represented in this equation. The average crystallite size of synthesized AgNPs was 14.43 nm, which was in good agreement with HR-TEM results.

Using HR-TEM, the morphological properties of GoBE-AgNPs were examined. Figure 4A-4D depicts the absence of aggregation and the evenly distributed smaller nanoparticles (20-27 nm range), spherical in shape and adorned with fringes. The size and shape of synthesized AgNPs ascribed with different antioxidant capacity and capping of bioactives present in the extract and the coating of a transparent organic layer surrounds the AgNP because, the presence of capping ingredients which prevent agglomeration (Sidhu et al., 2022). Figure 4E showed SAED patterns, which are consistent with the FCC structure of AgNPs, which correspond to the five diffraction rings: (111), (200), (220), (311), and (222). The bright spots indicated the crystalline orientation of AgNPs as discussed in the XRD results (Figure 3). Moreover, the exterior surface of the synthesized AgNPs was arranged with metallic elements, which was studied by EDS analysis, the strong electrical signals at 3 keV indicated the presence of Ag element. Other elements like oxygen and carbon were indicated at 0.1-0.5 keV, which may be bound to AgNPs during the extraction process (Figure 4F) (Ajitha et al., 2015).

The surface zeta potential in a hydrodynamic solution was used to analyze the surface charge stability of synthesized AgNPs. Figure 5A shows that the zeta value of AgNPs is -42.2 mV. As a negative side effect, it was found that the capping material effectively imparted intense negative charges during nanoparticle stabilization, preventing any nanoparticles from reaching the Riddick threshold (Riddick 1968). The particle size analyzer was utilized to ascertain the average particle size, size distribution profile, and polydispersity index (PDI) of the AgNPs that were produced was 0.684, as depicted in Figure 5B, the average size of the AgNPs was +40.7 nm. A relationship between the two results revealed that this method generated small-sized AgNPs with monodispersity in distribution (Priya et al., 2016).

Using ascorbic acid as a standard, the dose-dependent DPPH radical scavenging experiment revealed that AgNPs had a free-radical scavenging activity of 94.62±0.015% and the standard was 93.74±0.067% at higher concentration of 200 µg/ml. Compared to the standard, the synthesized AgNPs were potential free-radical scavengers (Figure 6). Similarly, the IC_{50} value of AgNPs showed 50.91 µg/ml and standard ascorbic acid showed 35.39 µg/ml (Table 1). Related to IC_{50} value, the synthesized AgNPs act as an effective antioxidant agent (Salari et al., 2019).

The anticancer activity of GoBE-AgNPs was tested against human bone marrow neuroblastoma cancer cells. At 200 µg/mL of AgNPs, after 24 hours of incubation, a noteworthy cell viability of 44.85±0.017 % and an effective IC_{50} concentration of 172.81 µg/mL was noted against the SH-SY5Y cell line. (Figure 7, Table 2). Because the capped bioactives present in the plant extract showed effective ability against cancer cells (Kalishwaralal et al., 2010). The crucial morphological changes like membrane blebbing were observed in SH-SY5Y cells due to the effective anticancer activity of AgNPs regulating the changes in apoptosis (Figure 8). GoBE-AgNPs significantly and dose-dependently caused apoptosis after a 24-hours of treatment period. Cell populations that were necrotic, non-apoptotic, and apoptotic were all controlled by Annexin V/PI. The result of staining confirm the significant induction of necrosis (Annexin V−/PI+) (0%, 0.72%, 6.82%), late apoptosis (Annexin V+/PI+) (2.4%, 29.34%, 50.54%) and early apoptosis (Annexin V+/PI−) (1.23%, 23.49%, 8.95%) in SH-SY5Y cells with different treatment groups such as untreated (negative control), camptothecin (positive control), and GoBE-AgNPs (test groups) at 12.5-200 µg/mL concentrations. (Figure 9, Figure 10). As compared to a positive control (52.83%), synthesized AgNPs (59.49%) effectively induced apoptosis in cancer cells, reducing the proportion of viable cells (Annexin V−/PI−). Increased Ag concentration, NP size, and efficient bioactive capping agents were among the variables contributing to the reduced cell viability and proliferation (Hsin et al., 2008). The fact that the synthesized AgNPs stimulate ROS production in SH-SY5Y cells. According to Gurunathan et al. (2013), the chemical transition of Ag+ ions from neutral silver (A°) is the usual mechanism for ROS creation. By generating intracellular ROS, the decreased non-fluorescent H2DCFDA can be converted into fluorescent DCF (Sabarwal et al., 2017). The DCF intensity was observed at M1 and M2 phases, as shown in figure 11, the GoBE-AgNPs treated with SH-SY5Y cells expressed 33.88% DCF intensity, while untreated-SH-SY5Y cells expressed 0.53% at positive M2 phase. Compared with untreated-SH-SY5Y cells, synthesized AgNPs dynamically increased (63.92-fold) the intracellular ROS production (Figure 12).

4. Conclusion

In current research, the therapeutically important plant *Guaiacum officinale* L. bark was investigated for green synthesis of silver nanoparticles. The preparation of hydroacetonic bark extract was carried out with a sophisticated ultrasonic-assisted extraction method. Hydroacetonic bark extract was used to synthesize the silver nanoparticles, further, the synthesized AgNPs were characterized by different analytical techniques. The phytochemicals capped on the nanoparticles' surface play a significant role in antioxidant and anticancer

activity. In the present study, GoBE-AgNPs were showed as an effective free radical scavenger and also a potential antioxidant agent. Synthesized AgNPs showed efficient cell viability to SH-SY5Y cell lines. The capability to induce apoptosis and generate oxidative stress through the production of reactive oxygen species in the SH-SY5Y cells validated that GoBE-AgNPs can be a potential medication for human bone marrow neuroblastoma cancer treatment.

5. Acknowledgment

The authors would like to express their sincere gratitude to – the Chairman, P. G. Department of Studies in Botany, Karnatak University, Dharwad, Karnataka, India, for the laboratory facility; to the USIC, SAIF-Dharwad, DST-PURSE Program Phase-II, Karnatak University, Dharwad, and Soniya Education Trust's College of Pharmacy, Dharwad, Karnataka, India for instrumental facilities. No funding was received for this research.

Conflict of interest

The authors declare no conflicts of interest.

6. References

Abou El-Nour, K. M., Eftaiha, A. A., Al-Warthan, A. and Ammar, R. A. (2010). Synthesis and applications of silver nanoparticles. *Arabian journal of chemistry*, *3*(3), 135-140.

Ahmed, S. M., Ahmed, S., Tasleem, F., Mohtasheem Ul Hasan, M. and Azhar, I. (2012). Acute Systemic Toxicity of Four Mimosaceous Plants Leaves In Mice. *IOSR Journal of Pharmacy*, *2*(2), 291–295.

Ajitha, B., Reddy, Y. A. K. and Reddy, P. S. (2015). Green synthesis and characterization of silver nanoparticles using Lantana camara leaf extract. *Materials science and engineering: C*, *49*, 373-381.

Alley, M. C., Scudiere, D. A., Monks, A., Czerwinski, M., Shoemaker, R. II. and Boyd, M. R. Validation of an automated microculture tetrazolium assay (MTA) to assess growth and drug sensitivity of human tumor cell lines. Proc. Am. Assoc. Cancer Res., 27: 389, 1986

Arya, G., Kumari, R. M., Gupta, N., Kumar, A., Chandra, R. and Nimesh, S. (2018). Green synthesis of silver nanoparticles using Prosopis juliflora bark extract: reaction optimization, antimicrobial and catalytic activities. *Artificial Cells, Nanomedicine and Biotechnology*, *46*(5), 985–993.

Behera, A. and Awasthi, S. (2021). Anticancer, antimicrobial and hemolytic assessment of zinc oxide nanoparticles synthesized from Lagerstroemia indica. *BioNanoScience*, *11*(4), 1030-1048.

Boholm, M. and Arvidsson, R. (2016). A Definition Framework for the Terms Nanomaterial and Nanoparticle. *NanoEthics*, *10*(1), 25–40.

Chandra, H., Kumari, P., Bontempi, E. and Yadav, S. (2020). Medicinal plants: Treasure trove for green synthesis of metallic nanoparticles and their biomedical applications. In *Biocatalysis and Agricultural Biotechnology* (Vol. 24).

Gurunathan, S., Han, J. W., Eppakayala, V., Jeyaraj, M. and Kim, J. H. (2013). Cytotoxicity of biologically synthesized silver nanoparticles in MDA-MB-231 human breast cancer cells. *BioMed research international*, *2013*.

Hsin, Y. H., Chen, C. F., Huang, S., Shih, T. S., Lai, P. S. and Chueh, P. J. (2008). The apoptotic effect of nanosilver is mediated by a ROS-and JNK-dependent mechanism involving the mitochondrial pathway in NIH3T3 cells. *Toxicology letters*, *179*(3), 130-139.

Hulkoti, N. I., and Taranath, T. C. (2014). Biosynthesis of nanoparticles using microbes—a review. *Colloids and surfaces B: Biointerfaces*, *121*, 474-483.

Jyoti D, P., Charu, A., Norah, L. H., Andrew, A., Christopher, F. and Glenn, L. (2022, June). *Neuroblastoma - Childhood: Introduction*. ASCO.Org

Kalishwaralal, K., Deepak, V., Pandian, S. R. K., Kottaisamy, M., BarathManiKanth, S., Kartikeyan, B. and Gurunathan, S. (2010). Biosynthesis of silver and gold nanoparticles using Brevibacterium casei. *Colloids and surfaces B: Biointerfaces*, *77*(2), 257-262.

Koopman, G., Reutelingsperger, C. P., Kuijten, G. A., Keehnen, R. M., Pals, S. T. and Van Oers, M. H. (1994). Annexin V for flow cytometric detection of phosphatidylserine expression on B cells undergoing apoptosis, 1415-1420.

Narayanan, K. B. and Sakthivel, N. (2011). Extracellular synthesis of silver nanoparticles using the bark extract of Coleus amboinicus Lour. *Materials Research Bulletin*, *46*(10), 1708–1713.

Nhung, T. T. and Lee, S. W. (2014). Green synthesis of asymmetrically textured silver meso-flowers (AgMFs) as highly sensitive SERS substrates. *ACS applied materials & interfaces*, *6*(23), 21335-21345.

Pandhari, R. and Taranath, T. C. (2024). In-vitro Antioxidant Activity and Flow Cytometric Analysis of Simarouba glauca DC Bark Extract Induced Apoptosis in Triple Negative Breast Cancer Cells. *Asian Pacific Journal of Cancer Prevention*, *25*(1), 201-210.

Priya, R. S., Geetha, D. and Ramesh, P. S. (2016). Antioxidant activity of chemically synthesized AgNPs and biosynthesized Pongamia pinnata leaf extract mediated AgNPs–A comparative study. *Ecotoxicology and environmental safety*, *134*, 308-318.

Ravichandra, V. D., Ramesh, C., Swamy, M. K., Purushotham, B. and Rudramurthy, G. R. (2018). Anticancer plants: chemistry, pharmacology, and potential applications. *Anticancer plants: Properties and Application: Volume 1*, 485-515.

Riddick, T., 1968. Control of colloid stability through zeta potential: with a closing chapter on its relationship to cardiovascular disease, Published for Zeta-Meter, inc., by Livingston Pub. Co.

Sabarwal, A., Agarwal, R. and Singh, R. P. (2017). Fisetin inhibits cellular proliferation and induces mitochondria-dependent apoptosis in human gastric cancer cells. *Molecular carcinogenesis*, *56*(2), 499-514.

Salari, S., Bahabadi, S. E., Samzadeh-Kermani, A. and Yosefzaei, F. (2019). In-vitro evaluation of antioxidant and antibacterial potential of green-synthesized silver nanoparticles using Prosopis farcta fruit extract. *Iranian journal of pharmaceutical research: IJPR*, *18*(1), 430.

Sidhu, A. K., Verma, N. and Kaushal, P. (2022). Role of biogenic capping agents in the synthesis of metallic nanoparticles and evaluation of their therapeutic potential. *Frontiers in Nanotechnology*, *3*, 801620.

Sulaiman, A. Z., Ajit, A., Yunus, R. M. and Chisti, Y. (2011). Ultrasound-assisted fermentation enhances bioethanol productivity. *Biochemical Engineering Journal*, *54*(3), 141-150.

Syahir, A., Sulaiman, S., Mel, M., Othman, M., & Zubaidah Sulaiman, S. (2020). An Overview: Analysis of ultrasonic-assisted extraction's parameters and its process. *IOP Conference Series: Materials Science and Engineering*, *778*(1).

Teng, H., Jo, I. H., & Choi, Y. H. (2010). Optimization of ultrasonic-assisted extraction of phenolic compounds from chinese quince (Chaenomeles sinensis) by response surface methodology. *Journal of Applied Biological Chemistry*, *53*(5), 618–625.

Xu, L., Wei, B., Liu, W., Zhang, H., Su, C. and Che, J. (2013). Flower-like ZnO-Ag2O composites: precipitation synthesis and photocatalytic activity. *Nanoscale research letters*, *8*, 1-7.

Cite this article as: Rangavitala, P. and Taranath, T. C. (2024) Green Synthesis of Guaiacum officinale L. Bark Extract Silver Nanoparticles Enhanced Anticancer Activity in Human Bone Marrow Neuroblastoma Cancer Cells. *Afr.J.Bio.Sc. 6(5) (2024). 1371-1389*. Doi: 10.33472/AFJBS.6.5.2024.1371-1389